energies

MDPI

Article

Process Modeling and Exergy Analysis for a Typical VOC Thermal Conversion Plant

Wencai Zhuo [1,2], Bin Zhou [1,*], Zhicheng Zhang [3], Hailiang Zhou [3] and Baiqian Dai [2,4,*]

[1] School of Energy and Environment, Southeast University, Nanjing 210042, China; wzhu0032@student.monash.edu
[2] Department of Chemical Engineering, Southeast-Monash Joint Graduate School, SIP, Suzhou 215123, China
[3] Suzhou Beyond Environmental Protection Technology Co., Ltd., Suzhou 215200, China; 13837143778@163.com (Z.Z.); 13401500707@139.com (H.Z.)
[4] Department of Chemical & Biological Engineering, Monash University, Melbourne, VIC 3800, Australia
* Correspondence: zhoubinde@seu.edu.cn (B.Z.); bai-qian.dai@monash.edu (B.D.)

Abstract: The emission of volatile organic compounds (VOCs) represents a major source of air pollution and presents a major risk to both the surrounding environment and local health. An efficient and clean VOCs conversion process is an important approach for energy conservation and emission reduction. In this work, process simulation is conducted using Aspen Plus according to a VOC thermal oxidizing plant for an industrial-scale aluminum spraying production process. Experimental measurements are used for model validation and the pollutant emissions are consistent with the actual plant operating parameters, where the concentration of sulfur oxides is 32 mg/m^3, and that of nitrogen oxides is ~34 mg/m^3, both of which are below the requirements specified by the national environment regulations in China. Energy and exergy analyses have been conducted from the perspective of the second law of thermodynamics. It is found that 68.8% of the output energy in the system considered here enters the subsequent oven production line, which will be reused for drying the aluminum plates, and the rest of the energy will contribute to the water heat exchanger; however, the furnace features the largest exergy loss of 34%, and this is due to the high-temperature heat loss. The water heat exchanger features 11.5% exergy loss, which is the largest for the series of heat exchangers, and this loss is due to the large temperature difference between the hot and cold streams in the water heat exchanger. These findings are expected to provide practical approaches to energy conservation from the perspective of energy management.

Keywords: VOCs; thermal conversion; process simulation; exergy analysis

Citation: Zhuo, W.; Zhou, B.; Zhang, Z.; Zhou, H.; Dai, B. Process Modeling and Exergy Analysis for a Typical VOC Thermal Conversion Plant. *Energies* **2022**, *15*, 3522. https://doi.org/10.3390/en15103522

Academic Editors: Po-Chih Kuo, Muhammad Aziz and Zhi-Yan (Rock) Du

Received: 1 April 2022
Accepted: 9 May 2022
Published: 11 May 2022

1. Introduction

Volatile organic compounds (VOCs) are a major source of air pollution that presents issues for the surrounding environment and local health. VOCs normally include benzene series compounds, organic chlorides, Freon products, organic ketones, amines, alcohols, esters, ethers, hydrocarbon compounds, etc. [1,2]. The emission of VOCs mainly occurs in fuel combustion, transportation, petrochemical processes, paint manufacturing, and other industrial processes. VOCs with irritating odors harm the human liver, kidneys, brain, and nervous system [3–5]. VOCs from industrial processes represent the main source of VOC emission and need thermal treatment to convert the harmful compounds to clean substances in a low energy consumption manner without secondary pollution [6]. Therefore, the appropriate approaches to control VOC emissions are not only related to the requirements from an environmental protection perspective, but also those that promote technological development for industrial processes [7,8]. The "VOC Pollution Prevention and Control Technology Policy", issued by the Chinese Environmental Protection Department in 2013, stipulates that the emission of VOCs from raw materials and products needs

to be strictly controlled during industrial production, especially in production processes related to fuel oil, coatings, and rubber products [9], where the maximum allowable emission concentration of toluene is 60 mg/m^3.

The emission of VOCs in industrial production is very common. It has been reported in a study of 600 MW coal-fired power plants that VOC emissions can reach approximately 0.00471–0.00134 kg/MWh when using fixed coal products [10,11]. A VOC thermal conversion process is an efficient method for removing volatile organic compounds. Through combustion, the VOC removal rate can reach 99% [12]. Another advantage of thermal conversion is that it can reduce nitrogen oxide emissions [13]. The temperature required for the direct oxidization of VOCs may be controlled to be below 800 °C, where thereby the formation of nitrogen oxides can be effectively controlled [14]. Preheaters can be designed in VOC thermal conversion processes to fully improve the thermal conversion efficiency [15]. Studies have analyzed the influence of intake airflow on thermal efficiency by one-dimensional dynamic modeling of direct VOC combustion [16]. Studies on the removal of volatile organic compounds by dielectric barrier discharge and low-temperature plasma techniques also exist [17]. Recently, there have been studies on the establishment of mathematical models for VOC physical adsorption processes. Based on the removal of VOCs in building materials, boundary conditions have been set to evaluate the periodic changes related to the hexanal concentration in the indoor air [18,19]. In related research on thermal conversion processes for VOCs, most works focus on the exploration of the combustion characteristics of catalysts from an experimental perspective. So far, modeling works have only touched on physical adsorption processes for VOCs, and study on the thermal conversion of VOCs is limited in terms of modeling. Researchers have used partial differential equations to numerically simulate the combustion processes of VOCs alongside catalysts [20,21]. Few studies exist on models that can truly and accurately reflect direct oxidation processes for VOCs regarding thermal conversion. There are rarely studies on the evaluation of efficiency for VOCs thermal conversion processes from the energy and exergy perspective.

This work targets on an industrial-scale plant for a VOC thermal oxidization process that features an environmental treatment process for a color aluminum spraying production line with an airflow rate of 20,000 m^3/h. Process simulation and energy analysis have been conducted using Aspen Plus. Sensitivity analysis has been conducted by varying the fuel flow rate and temperature in the furnace. The predictions for the emissions have been validated by experimental measurement. The findings were expected to provide theoretical reference and practical support to improve the efficiency of the VOCs thermal conversion processes.

2. Methodology

2.1. Process Modeling

The basic model process and parameters were selected from a color aluminum spraying factory located in Anhui, China. The factory covers an area of 200,000 square meters and has four color aluminum spraying production lines. Aluminum flake spraying paints and reactants generate VOCs, including benzene series compounds and alkanes with concentrations ranging from 500–5000 mg/m^3 within air flowing at a rate of 20,000 m^3/h. A thermal oxidization process was designed to burn the VOCs with methane fuel with a consumption of 3000 m^3/day. Figure 1 shows the general flow path of the VOC thermal conversion process. It is mainly composed of four components, namely, a furnace and three heat exchangers. The feed inlet is divided into two sides. The VOC stream includes the air carrying volatile organic compounds, which come from the sorbent vaporization during the aluminum plate drying process. Methane is the fuel for the furnace, where the air carries the methane into the combustion area and acts as the fuel for the furnace. After the VOC heat treatment process in the combustion chamber, the high-temperature flue gas passes through three heat exchangers for energy recovery and utilization. The hot air system separates a certain proportion of the flue gas after passing through the

medium temperature heat exchanger and enters the oven system. The setting of the water heater adds an energy output port to the system by increasing the water temperature. After passing through the water heater, the flue gas is disposed of through the chimney.

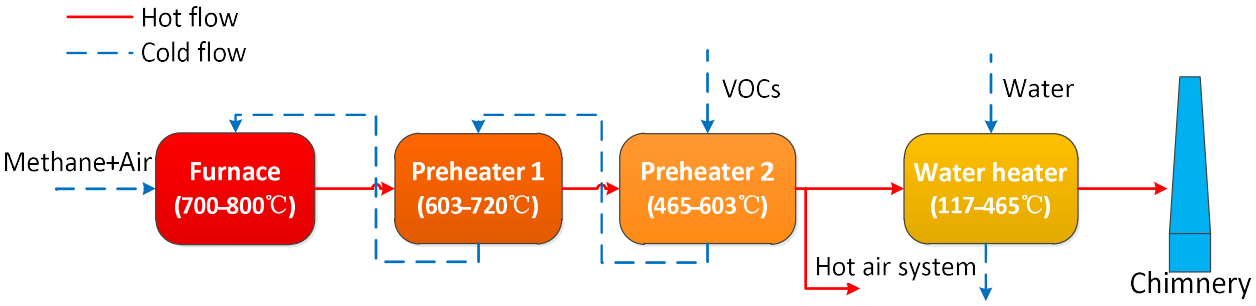

Figure 1. Volatile organic compound (VOC) thermal conversion flow chart.

The Gibbs free energy minimization principle has been used in this work to ensure that the reactants are all burned under the premise of an excessive oxygen concentration. The working fluids used, including toluene, methane, and air, have all been sourced from Aspen Plus. The concentration of nitrogen oxides in the exhaust gas has been measured as defined by the HJ 693–2014 standard, and that of sulfur oxides has been measured by as defined by the HJ 57–2017 standard [22,23].

2.2. System Parameter Determination

The feed parameters of the model are shown in Table 1, where the VOC concentration is set as 5000 mg/m^3, and the methane consumption in the combustion-supporting air is 120 m^3/h.

Table 1. Feeding parameters.

Parameter		Value
VOC concentration (mg/m^3)		5000
Water consumption (m^3/h)		20
VOC inlet	VOC consumption (m^3/h)	22.43
	Air consumption (m^3/h)	20,000
Combustion inlet	Methane consumption (m^3/h)	120
	Air consumption (m^3/h)	2500

The operating temperature parameters of the heat exchanger are shown in Table 2. The temperature of the VOCs at the inlet is 220 °C. The air at room temperature carries the methane into the combustor. After the combustion and heat exchange processes, the hot air, with a temperature of 465 °C, is reused in the production line and the flue gas is exhausted through the chimney after moving through the water heat exchanger.

Table 2. Heat exchanger temperature parameters.

	High Temperature Preheater	Medium Temperature Preheater	Water Heater
Heat flow (°C)	720 → 603	603 → 465	465 → 117
Cold flow (°C)	385 → 523	220 → 385	25 → 70

The compositions of VOCs are shown in Table 3. Methane concentration in combustion inlet varies with the calorific value of VOCs.

Table 3. Compositions for VOCs.

VOCs	Mass Percentage (%)
Octane	9.97
1-Butene	0.84
Benzene	1.47
Toluene	30.22
Ethylbenzene	19.07
Para-xylene	11.87
Styrene	11.03
Ortho-xylene	11.07
N-propylbenzene	3.93
Methyl mercaptan	0.22
Hydrogen sulfide	0.31
Total	100

2.3. Exergy Analysis

In this paper, the calculation of exergy is shown in Formula (1), where only physical exergy and chemical exergy are considered [24].

$$E = E_{ph} + E_{ch} \tag{1}$$

where E_{ph} is physical exergy and E_{ch} is chemical exergy. Physical exergy occurs when the system has a pressure difference and a temperature difference between the system and the standard state. At this time, the system is in an incomplete equilibrium state. The standard condition of this work is 25 °C at 101.325 kPa, as shown in Formula (2):

$$E_{ph} = (H - H_0) - T_0(S - S_0) \tag{2}$$

where H is the enthalpy of steady flow material; H_0 is enthalpy value of material under standard conditions; S is entropy value of steady flow material; S_0 is entropy value of material under standard conditions. For the chemical exergy of the materials in the process, the chemical exergy calculation formula of the mixture can be used for calculation as shown in Formula (3):

$$e_{ch} = \sum x_i e_i + RT_0 \sum (x_i \ln x_i) \tag{3}$$

where x_i is the mole fraction of each component of the mixture and e_i is the standard chemical exergy of each component. The standard chemical exergy of a single carbon oxyhydroxide can be calculated based on the content of the component carbon, hydrogen, and oxygen, as shown in Formula (4):

$$e_{ch} = ae_{ch,C} + \frac{b}{2}e_{ch,H_2} + \frac{c}{2}e_{ch,O_2} + (\Delta G_f^0)_{C_aH_bO_c} \tag{4}$$

where $(\Delta G_f^0)_{C_aH_bO_c}$ is Gibbs free generating energy of standard formation of the compound. The standard Gibbs free generating energy of a single compound can be checked from the Aspen Plus physical property library. The exergy efficiency of the system refers to the ratio of output exergy value to input exergy value, as shown in Formula (5):

$$\eta = \frac{E_O}{E_I} \tag{5}$$

where E_O is system output exergy, including exergy for water heater and hot air, and E_I is system input exergy [25].

3. Results and Discussion

3.1. Process Simulation and Validation

Figure 2 provides a flowsheet of the thermal conversion process for VOCs. The inputs and key parameters were those of the industrial process and the emission was measured by an onsite experiment. Predictions of NOx and SOx were selected for validation as they are the key concerns from an environmental perspective.

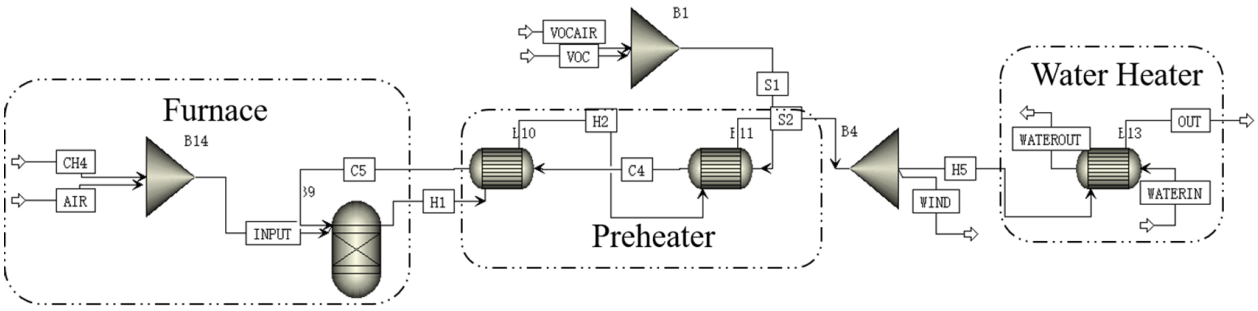

Figure 2. Flow diagram of the thermal conversion of VOCs.

Sulfur oxides are exhaust gases that are mainly composed of sulfur dioxide and sulfur trioxide, which is produced by the combustion of sulfur-containing substances such as methyl mercaptan in the VOCs. Nitrogen oxides contain nitrogen monoxide and nitrogen dioxide, which are produced from the furnace during high temperature combustion. Figure 3 provides the SOx and NOx concentration in the exhaust, where the results are compared between the model and onsite measurement values. The local regulations of air pollutant emissions for these two components are listed for comparison as well. The results of the modeling prediction are consistent with those measured in the actual process, where both are around 33 mg/m^3. According to the relevant regulations of GB 13271–2014, "Emission Standard of Air Pollutants for Boiler", the highest emission concentration of sulfur oxides should be lower than 50 mg/m^3, and that of nitrogen oxides should be lower than 150 mg/m^3 [26]. This means that the emission of VOCs from the process is much lower than the regulation standard describes, indicating that a highly efficient conversion was achieved in the process.

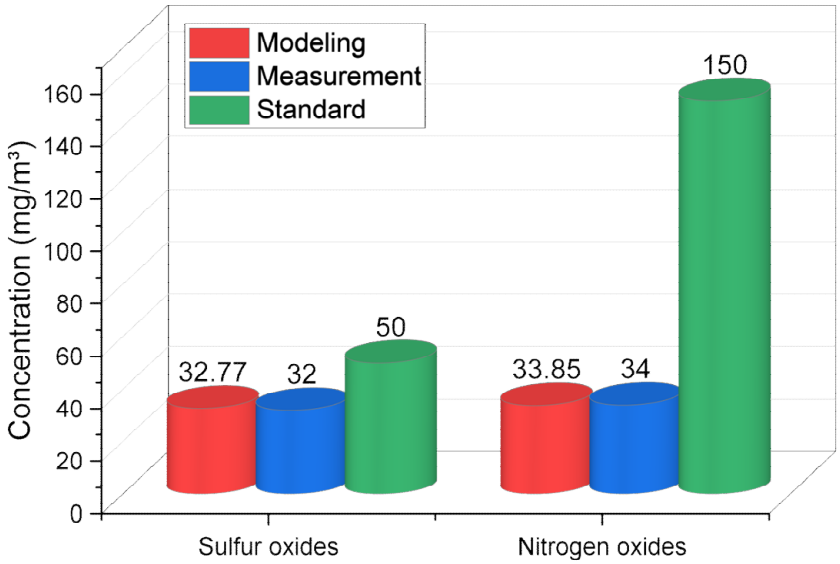

Figure 3. Concentration of sulfur oxides and nitrogen oxides in the exhaust.

To provide detailed information on the nitrogen oxides and sulfur oxides in the emission, Figure 4 shows the types of main components in nitrogen oxides and sulfur

oxides, among which NO accounts for the largest proportion of nitrogen oxides, and sulfur oxides mainly include SO_2 and SO_3. NOx and SOx accounted for half of the pollutants, among which NO accounted for the largest proportion with 47.1%, and SO_2 and SO_3 accounted for 24.0% and 25.1% respectively.

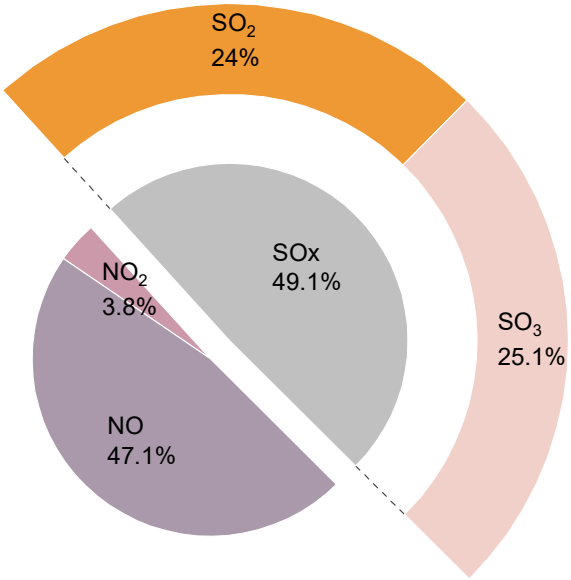

Figure 4. Composition for the pollutants.

3.2. Energy Balance and Energy Distribution of the Process

The energy input of the feedstocks comes from fuel for the furnace and the VOC components, which are normally hydrocarbons with large heating values. The VOCs compounds from the aluminum production line were carried by the hot air before entering the furnace, while the fuel was the methane, which provides sufficient heat for VOC combustion in the furnace. The heating values from feedstocks are listed in Table 4. The output of the energy distribution process was analyzed, which was carried by hot flue gas and experienced heat exchange before entering the aluminum production line, and a portion of the flue gas was exhausted through the chimney after passing through the water heat exchanger.

Table 4. Heating values for the feedstocks.

Parameter	Heating Value (kJ/mol)
Methane	802.62
Toluene	3734
Benzene	3136
Para-xylene	4331.8
Ortho-xylene	4333
Ethylbenzene	4344.8
Styrene	4219
Octane	5074.15
N-propylbenzene	4954.15
1-Butene	2540.8
Methyl mercaptan	1151.7
Hydrogen sulfide	518

The energy flow of each part is calculated as per Formula (6):

$$\Delta Q = Q_{out} - Q_{in} = m(Hm_{out} - Hm_{in}) \quad (6)$$

where m is molar flow and Hm is molar enthalpy of the inlet and outlet fluids.

Figure 5 shows a diagram of energy flow for the whole system. In the two parts of the system input energy, VOC accounted for 66.6% more than methane. The energy loss between inlet and outlet parts only accounted for 7.4%, mainly including the heat dissipation of the furnace and the heat loss of the flue gas. Furnace heat dissipation occurred because the methane provided more energy than that required for the furnace, and the excess energy was released in the form of heat dissipation. The flue gas heat loss was the difference between the enthalpy of flue gas through the chimney and was of ideal standard conditions. As for the output energies of this system, the hot air parts accounted for 68.8%, which is the largest proportion.

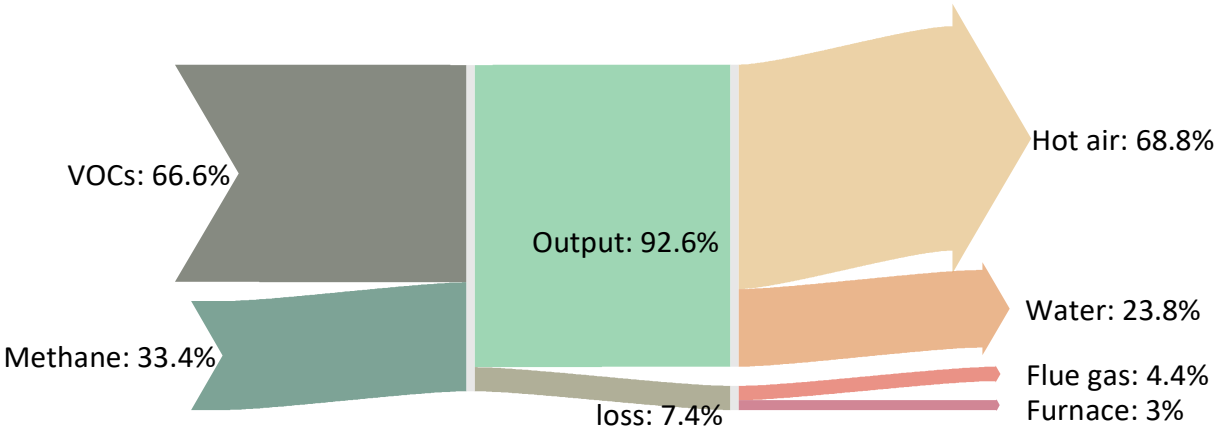

Figure 5. Flow diagram of energy distribution.

3.3. Exergy Flow Analysis

After evaluating the energy balance and the distribution of the process, exergy analysis was conducted to examine the valuable energy that can be further utilized for the system. Figure 6 provides an exergy diagram of the process which is aligned with the energy distribution in Figure 5.

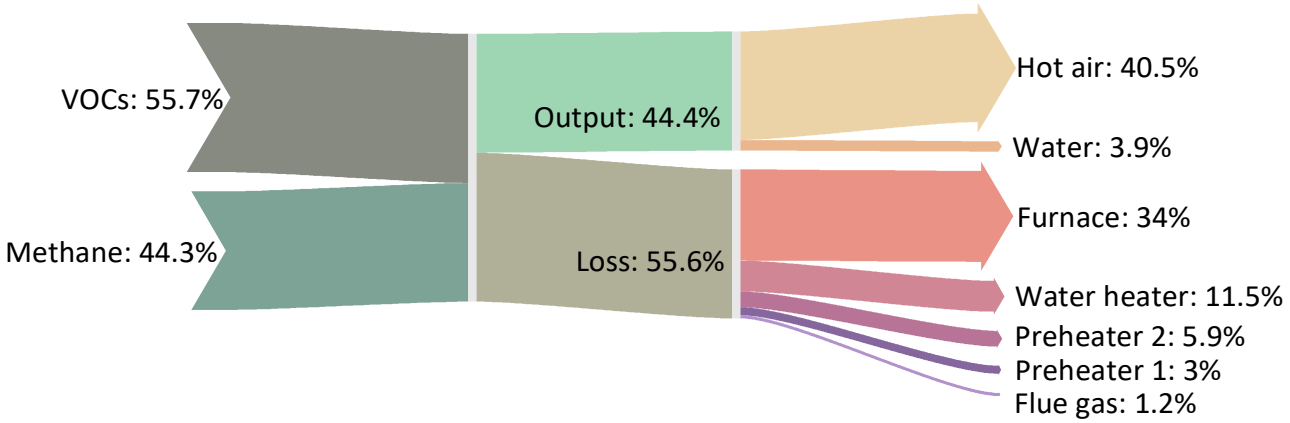

Figure 6. Flow diagram of exergy distribution.

The exergy flow of the system is divided into two parts, namely, exergy output, and exergy loss, accounting for 44.4% and 55.6%, respectively. The hot air exergy, with a proportion of 40.5%, is the primary output of this system. As for exergy loss, the furnace, with the highest temperature in the whole process, has the largest exergy loss and is as high as 34%. Apart from the furnace, the water heat exchanger has an exergy loss of 12%, which is the largest of the heat exchangers. This is because the heat exchange temperature difference of the water heater is larger, and its output product is only used for preheating and washing aluminum sheets. Therefore, the exergy loss will be higher than preheater 1 and preheater 2, which conforms to the principle that a greater temperature difference

incurs a greater exergy loss. As such, shortening the temperature gap between the cold and hot streams for the water heat exchanger will decrease the exergy loss and improve the exergy efficiency.

3.4. Sensitivity Analysis

Sensitivity analysis has been conducted to further investigate the process capability in terms of fuel adaptability, emissions, and efficiency. As methane is the fuel that determines the energy consumption of the system and directly reflects the cost of the process. The sensitivity analysis selected the methane flow rate as the independent variable, where the input flow rate of methane varied from 100 m^3/h to 140 m^3/h with a step size of 1 m^3/h for the sensitivity analysis. The key factors included the water heater outlet temperature, exhaust nitrogen oxide, sulfide concentration, and exergy efficiency, which were selected as dependent variables to examine the tolerance during the methane variation range.

The temperature of the furnace is the key factor that affects the process efficiency and stability. Therefore, sensitivity analysis was first conducted by varying the furnace temperature. In Figure 7, the furnace temperature was selected as the independent variable, and the pollutant concentration, which was the main concern for emission was selected as dependent for the sensitivity analysis. It was found that with an increase in the furnace temperature, the overall concentration of pollutants increased significantly, especially the concentration of NO, which increased from 22.34 mg/m^3 to 66.95 mg/m^3 as the temperature increased from 700 °C to 780 °C. The concentration of SO_3 decreased slightly, but the decreased magnitude was lower than that of the increase of SO_2 concentration. The concentration of SO_2 increased by 10.91 mg/m^3, but that of SO_3 decreased by 4.34 mg/m^3. As the temperature increased, the rate of redox reaction between nitrogen and oxygen will be promoted, resulting in an increase for the concentration of nitrogen oxides. Sulfur oxides mainly came from the sulfur-containing organics in the VOCs, where the rate of redox reactions is promoted as the temperature increases, resulting in an increase in the SOx concentration in the flue gas [27].

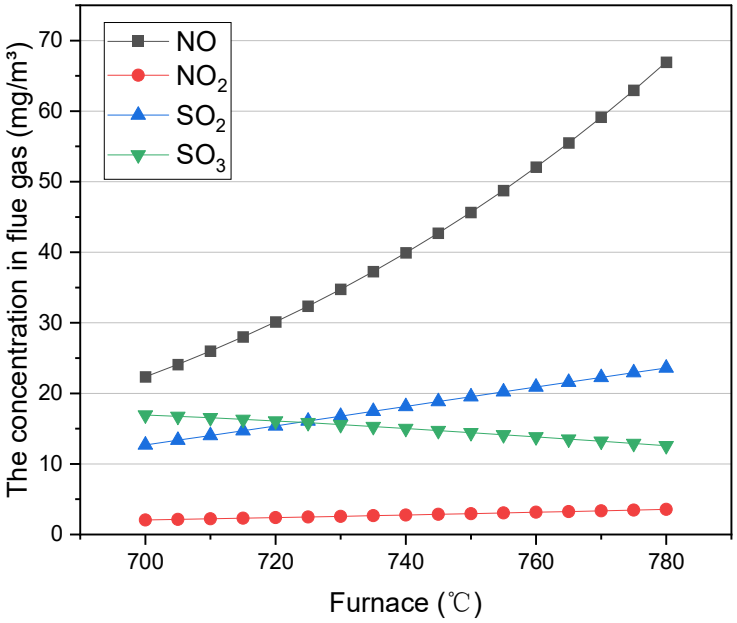

Figure 7. Sensitivity analysis as the function of furnace temperature.

As shown in Figure 8, to meet the temperature demand of the water heater outlet, the amount of methane in the combustion-supporting air needs to be continuously increased and can only heat water to 68.4 °C at 100 m^3/h and 83.5 °C at 140 m^3/h. Meanwhile, with the continuous increase of the amount of methane, the pollutants in the exhaust increase, and the exergy efficiency decreases linearly. The concentration of NOx and SOx increased

by 40.98 mg/m^3 and 4.28 mg/m^3 as the volume flow of methane increased from 100 m^3/h to 140 m^3/h. An increase in the amount of fuel will result in a higher temperature in the furnace, which results in larger amounts of pollutant emission, especially nitrogen oxides. The exergy efficiency of this system is the ratio of the exergy revenue to the input exergy, which decreases from 42.03% to 31.22% with increasing methane volume flow rates.

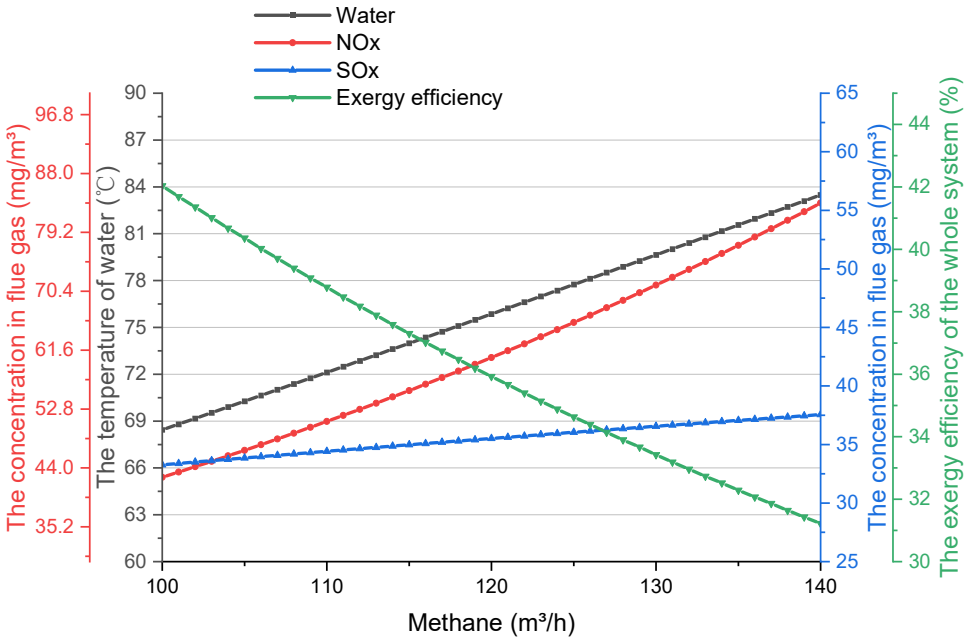

Figure 8. Sensitivity analysis as the function of flowrate of methane.

4. Conclusions

In summary, a direct thermal conversion process for VOCs in a color aluminum spraying plant has been accurately simulated using Aspen Plus in this paper. Energy flow analysis has been employed for the process flowsheet, where the energy distribution for the thermal process is visualized by quantification. The key pollutants in the emission, including NOx and SOx, have been validated by in situ measurement, where the prediction results match the experimental measurements well. The hot air stream, which is the reused heat source, represented the greatest energy with a proportion of 68.8%, indicating an effective process design in terms of energy conservation. Furthermore, exergy analysis from the perspective of the second law of thermodynamics has been conducted for the process to examine the energy qualities of each unit. The exergy loss for the furnace was the biggest, representing 34% of the total exergy loss. Additionally, the exergy loss of the water heat exchanger was larger than the rest of heat exchangers, with a proportion of 11.5%, which is due to the larger heat exchange temperature difference between the cold and hot streams. The sensitivity analysis for the process indicates that the supply of methane could influence the pollutant emissions of the system. With an increase in the methane volume flow rate from 100 m^3/h to 140 m^3/h, the concentration of NOx and SOx increased by 30.98 mg/m^3 and 4.28 mg/m^3, and the exergy efficiency decreased from 42.03% to 31.22%.

Author Contributions: Conceptualization, B.Z.; Data curation, Z.Z. and H.Z.; Supervision, B.D.; Writing—original draft, W.Z. All authors have read and agreed to the published version of the manuscript.

Funding: This research received no external funding.

Data Availability Statement: All data generated or analyzed during this study are included in this published article.

Acknowledgments: The authors grateful for the experimental support from Wonderful-wall color coating Aluminum (Anhui).

Conflicts of Interest: The authors declare that there are no conflicts of interest for this publication.

References

1. Li, G.; Wei, W.; Shao, X.; Nie, L.; Wang, H.; Yan, X.; Zhang, R. A comprehensive classification method for VOC emission sources to tackle air pollution based on VOC species reactivity and emission amounts. *J. Environ. Sci.* **2018**, *67*, 78–88. [CrossRef] [PubMed]
2. Zhang, K.; Li, L.; Huang, L.; Wang, Y.; Huo, J.; Duan, Y.; Wang, Y.; Fu, Q. The impact of volatile organic compounds on ozone formation in the suburban area of Shanghai. *Atmos. Environ.* **2020**, *232*, 117511. [CrossRef]
3. Kim, S.; Kim, H.-J.; Moon, S.-J. Evaluation of VOC Emissions from Building Finishing Materials Using a Small Chamber and VOC Analyser. *Indoor Built Environ.* **2006**, *15*, 511–523. [CrossRef]
4. You, Z.; Zhu, Y.; Jang, C.; Wang, S.; Gao, J.; Lin, C.-J.; Li, M.; Zhu, Z.; Wei, H.; Yang, W. Response surface modeling-based source contribution analysis and VOC emission control policy assessment in a typical ozone-polluted urban Shunde, China. *J. Environ. Sci.* **2017**, *51*, 294–304. [CrossRef] [PubMed]
5. Farzad, D.; Davood, K. Health risk assessment of VOC emissions in laboratory rooms via a modeling approach. *Environ. Sci. Pollut. Res. Int.* **2018**, *25*, 18.
6. Lim, M.; Lea-Langton, A.R. Investigation of Non-thermal Plasma Assisted Combustion of Solid Biomass Fuels: Effects on Flue Gas Composition and Efficiency. *Plasma Chem. Plasma Process.* **2020**, *40*, 1465–1483. [CrossRef]
7. Chen, Y.; Liao, Y.; Chen, L.; Chen, Z.; Ma, X. Performance of transition metal (Cu, Fe and Co) modified SCR catalysts for simultaneous removal of NO and volatile organic compounds (VOCs) from coal-fired power plant flue gas. *Fuel* **2020**, *289*, 119849. [CrossRef]
8. Jarczewski, S.; Barańska, K.; Drozdek, M.; Michalik, M.; Bizon, K.; Kuśtrowski, P. Energy-balanced and effective adsorption-catalytic multilayer bed system for removal of volatile organic compounds. *Chem. Eng. J.* **2022**, *431*, 133388. [CrossRef]
9. Zhu, M.; Huang, H.; Wang, Y.; Huang, Z.; Zhang, X.; Tang, M.; Lu, M.; Chen, C.; Shi, B.; Chen, Z.; et al. A newly integrated dataset of volatile organic compounds (VOCs) source profiles and implications for the future development of VOCs profiles in China. *Sci. Total Environ.* **2021**, *793*, 148348.
10. Peng, Y.; Yang, Q.; Wang, L.; Wang, S.; Li, J.; Zhang, X.; Zhang, S.; Zhao, H.; Zhang, B.; Wang, C.; et al. VOC emissions of coal-fired power plants in China based on life cycle assessment method. *Fuel* **2021**, *292*, 120325. [CrossRef]
11. Yan, Y.; Peng, L.; Li, R.; Li, Y.; Li, L.; Bai, H. Concentration, ozone formation potential and source analysis of volatile organic compounds (VOCs) in a thermal power station centralized area: A study in Shuozhou, China. *Environ. Pollut.* **2017**, *223*, 295–304. [CrossRef]
12. Kim, E.H.; Chun, Y.N. VOC decomposition by a plasma-cavity combustor. *Chem. Eng. Process. Process Intensif.* **2016**, *104*, 51–57. [CrossRef]
13. Veerapandian, S.K.P.; Leys, C.; De Geyter, N.; Morent, R. Abatement of VOCs Using Packed Bed Non-Thermal Plasma Reactors: A Review. *Catalysts* **2017**, *7*, 113. [CrossRef]
14. Salvador, S.; Commandre, J.-M.; Kara, Y. Thermal recuperative incineration of VOCs: CFD modelling and experimental validation. *Appl. Therm. Eng.* **2006**, *26*, 2355–2366. [CrossRef]
15. Bedi, U.; Chauhan, S. Modeling the combustion of volatile organic compound (VOC) ethane in monolithic catalytic converter. *Mater. Today Proc.* **2020**, *28*, 1727–1731. [CrossRef]
16. Frigerio, S.; Mehl, M.; Ranzi, E.; Schweiger, D.; Schedler, J. Improve efficiency of thermal regenerators and VOCs abatement systems: An experimental and modeling study. *Exp. Therm. Fluid Sci.* **2006**, *31*, 5. [CrossRef]
17. Li, S.; Dang, X.; Yu, X.; Abbas, G.; Zhang, Q.; Cao, L. The application of dielectric barrier discharge non-thermal plasma in VOCs abatement: A review. *Chem. Eng. J.* **2020**, *388*, 124275. [CrossRef]
18. Deng, B.; Zhang, H.; Wu, J. Modeling VOCs emission/sorption with variable operating parameters and general boundary conditions. *Environ. Pollut.* **2021**, *271*, 116315. [CrossRef]
19. Mocho, P.; Desauziers, V.; Plaisance, H.; Sauvat, N. Improvement of the performance of a simple box model using CFD modeling to predict indoor air formaldehyde concentration. *Build. Environ.* **2017**, *124*, 450–459. [CrossRef]
20. Rui, Z.; Lu, Y.; Ji, H. Simulation of VOCs oxidation in a catalytic nanolith. *RSC Adv.* **2012**, *3*, 1103–1111. [CrossRef]
21. Bedi, U.; Chauhan, S. Mathematical modeling of automotive catalytic converter for catalytic combustion of the volatile organic compound (voc) methane. *J. Phys. Conf. Ser.* **2020**, *1706*, 012035. [CrossRef]
22. National Environmental Protection Standard of the People's Republic of China HJ 693-2014; Stationary Source Emission-Determination of Nitrogen Oxides-Fixed Potential by Electrolysis Method. 2014. Available online: https://www.mee.gov.cn/ywgz/fgbz/bz/bzwb/jcffbz/201402/t20140217_267824.htm (accessed on 8 May 2022).
23. National Environmental Protection Standard of the People's Republic of China HJ 57-2017; Stationary Source Emission-Determination of Sulfur Dioxide-Fixed Potential by Electrolysis Method. 2017. Available online: https://www.mee.gov.cn/ywgz/fgbz/bz/bzwb/jcffbz/201712/t20171207_427551.shtml (accessed on 8 May 2022).
24. Dai, B.; Zhang, L.; Cui, J.-F.; Hoadley, A.; Zhang, L. Integration of pyrolysis and entrained-bed gasification for the production of chemicals from Victorian brown coal—Process simulation and exergy analysis. *Fuel Process. Technol.* **2017**, *155*, 21–31. [CrossRef]

25. Behbahaninia, A.; Ramezani, S.; Hejrandoost, M.L. A loss method for exergy auditing of steam boilers. *Energy* **2017**, *140*, 253–260. [CrossRef]
26. National Standards of the People's Republic of China GB 13271-2014; Emission Standard of Air Pollutants for Boiler. 2014. Available online: https://www.mee.gov.cn/ywgz/fgbz/bz/bzwb/dqhjbh/dqgdwrywrwpfbz/201405/t20140530_276318.shtml (accessed on 8 May 2022).
27. Alsultan, A.G.; Mijan, N.A.; Mansir, N.; Razali, S.Z.; Yunus, R.; Taufiq-Yap, H.Y. Combustion and Emission Performance of CO/NOx/SOx for Green Diesel Blends in a Swirl Burner. *ACS Omega* **2021**, *6*, 408–415. [CrossRef]